

# Rational engineering of a multi-step biocatalytic cascade for the conversion of cyclohexane to polycaprolactone monomers in *P. taiwanensis*

Lisa Schäfer<sup>1</sup>, Katja Bühler<sup>2</sup>, Rohan Karande<sup>1</sup>, and Bruno Bühler<sup>1</sup>

<sup>1</sup>Helmholtz Centre for Environmental Research

<sup>2</sup>Helmholtz-Centre for Environmental Research - UFZ

May 26, 2020

## Abstract

The current industrial production of polymer building blocks such as  $\epsilon$ -caprolactone ( $\epsilon$ -CL) and 6-hydroxyhexanoic acid (6HA) is a multi-step process associated with critical environmental issues such as the generation of toxic waste and high energy consumption. Consequently, there is a demand for more eco-efficient and sustainable production routes. This study deals with the generation of a platform organism that converts cyclohexane to such polymer building blocks without the formation of byproducts and under environmentally benign conditions. Based on kinetic and thermodynamic analyses of the individual enzymatic steps, we rationally engineered a 4-step enzymatic cascade in *Pseudomonas taiwanensis* VLB120 via stepwise biocatalyst improvement on the genetic level. We found that the intermediate product cyclohexanol severely inhibits the cascade and optimized the cascade by enhancing the expression level of downstream enzymes. The integration of a lactonase enabled exclusive 6HA formation without side products. The resulting biocatalyst showed a high activity of  $44.8 \pm 0.2 \text{ U g}_{\text{CDW}}^{-1}$  and fully converted 5 mM cyclohexane to 6HA within 3 h. This platform organism can now serve as a basis for the development of greener production processes for polycaprolactone and related polymers.

## 1 Introduction

Nature has assembled a multitude of microbial metabolic pathways constituting highly efficient reaction cascades that have been optimized during evolution<sup>[1]</sup>. In synthetic applications, cascade reactions allow for streamlined product formation via multiple reaction steps with the advantage to avoid the isolation of intermediates, thus saving resources, reagents, and time<sup>[2]</sup>. Although the balancing of enzyme ratios *in vivo* is more complicated than *in vitro*, multi-step biocatalysis employing whole cells emerged as a powerful tool for the synthesis of value-added compounds<sup>[1, 3]</sup>. Precise and delicate fine-tuning of gene expression is required to balance individual enzyme amounts and activities for the construction of “designer cells”<sup>[2, 4]</sup>. Especially “artificial cascades” employing heterologous genes of diverse origin constitute a major challenge as they introduce novel enzymatic functions into the host<sup>[5]</sup>. On the one hand, it is crucial to provide sufficient enzyme amounts to sustain reasonable rates. On the other hand, too much overexpression, especially of more than one gene, can severely hamper host metabolism and interfere with its stability<sup>[6, 7]</sup>. A drain of resources from the central metabolism may affect overall enzyme resynthesis, cofactor supply, as well as enzyme folding and consequently cascade efficiency. Also, optimizations regarding the choice of the host strain, substrate uptake and flux can provide a systematic understanding of the *in vivo* cascade<sup>[7-9]</sup>. A holistic approach comprising catalyst and reaction engineering allows controlling the product formation patterns<sup>[10]</sup>.

Nowadays, plastics are ubiquitous in human life and cause severe litter problems. Thus, biodegradable polymers such as poly-caprolactone (PCL), polylactic acid, and polyhydroxyalkanoate have gained importance<sup>[11]</sup>.

PCL can either be synthesized by the ring-opening polymerization of  $\epsilon$ -caprolactone ( $\epsilon$ -CL) or by the polycondensation of 6-hydroxyhexanoic acid (6-HA)<sup>[12]</sup>. Industrially,  $\epsilon$ -CL is produced from cyclohexane through the Union Carbide Corporation (UCC) process, which suffers from serious environmental issues, a low cyclohexane conversion of 10-12 %, and only moderate selectivity of 85-90 %<sup>[13, 14]</sup>. Recently, two biocatalytic approaches to synthesize  $\epsilon$ -CL from cyclohexane have been published. Pennec *et al.* demonstrated a one-pot reaction applying purified enzymes<sup>[15]</sup>, whereas Karande *et al.* generated a whole-cell biocatalyst showing superior total turnover numbers<sup>[16]</sup>. Especially, the involvement of oxidoreductases constitutes a major challenge, as reasonable *in vivo* oxidoreductase activities depend on high expression levels of the active enzyme<sup>[17]</sup>.

Karande *et al.* established a three-step cascade in *P. taiwanensis* VLB120 by introducing cytochrome P450 monooxygenase (Cyp), cyclohexanol dehydrogenase (CDH), and Baeyer-Villiger cyclohexanone monooxygenase (CHMO) genes from *Acidovorax* sp. CHX100 (Figure 1). Respective cascade development mainly focused on the monomer  $\epsilon$ -CL and gave rise to a maximal activity of 22 U g<sub>CDW</sub><sup>-1</sup>. Thereby, the first enzyme – the Cyp turned out to be rate-limiting ( $\sim$ 20 U g<sub>CDW</sub><sup>-1</sup>). The successive enzymes, the CDH, and the CHMO exhibited much higher activities of 80 U g<sub>CDW</sub><sup>-1</sup> and 170 U g<sub>CDW</sub><sup>-1</sup>, respectively. In a separate study, the activity of cells containing only the Cyp could be more than doubled by expression system engineering<sup>[18]</sup>. A combination of this system with CDH and CHMO should guarantee high respective activities to prevent the accumulation of intermediates and, at the same time, keep the expression related metabolic burden reasonably low to allow for stable catalysis. Explicitly, oxygenases such as Cyps or Bayer-Villiger monooxygenases are prone to form reactive oxygen species via uncoupling reactions, which may hamper the catalytic prowess of the cells<sup>[7, 9]</sup>. Another point to be considered is that, due to the accumulation of the hydrolysis product 6HA, the approach of Karande *et al.*<sup>[16]</sup> suffered from restricted cascade selectivity. This study aimed at the optimization of this *in vivo* cascade by rational pathway engineering including the characterization of the involved enzymes as the basis for the rational assembly of the expression system. It is thereby crucial to balance enzyme activities without dissipating the cell's resources.

## 2 Materials and methods

### 2.1 Bacterial strains, plasmids, media, and chemicals

Microbial strains and plasmids used in this work are listed in Table S1. Cells were grown in lysogeny broth (LB) medium<sup>[19]</sup> or M9\* medium<sup>[20]</sup> with a pH of 7.2 supplemented with 0.5 % (w/v) glucose as sole carbon and energy source. Kanamycin (50  $\mu$ g mL<sup>-1</sup>) was applied for selection when necessary. Unless stated otherwise, all chemicals were purchased from Sigma-Aldrich (Steinheim, Germany) or Carl Roth (Karlsruhe, Germany) in the highest purity available and used without further purification. 6HA was acquired from aber (Karlsruhe, Germany). Molecular biology methods and strain constructions are explained in detail in the Supplementary Information (Sections 1 and 2)

### 2.2 Growth of bacterial cultures

Cultivations were carried out at 30 °C and 200 rpm in a Multitron shaker (Infors, Bottmingen, Switzerland). Microorganisms were cultivated in an LB pre-culture for ca. 20 h, from which an M9\* pre-culture (1% v/v) was inoculated and incubated for another 12-16 h. From this culture, an M9\* main culture was inoculated to a starting OD<sub>450</sub> of 0.2. Heterologous gene expression was induced with 1 mM isopropyl  $\beta$ -d-1-thiogalactopyranoside (IPTG) when the cultures reached an OD<sub>450</sub> of  $\sim$ 0.5. Incubation was continued for another 4-6 h, and cells were harvested for SDS-PAGE analyses, CO spectra analyses, and/or activity or toxicity assays (see below).

### 2.3 Toxicity assay

*P. taiwanensis* VLB120 was cultivated as described above but without induction. Different concentrations of  $\epsilon$ -CL or 6HA were added 2 h after inoculation, and the growth rate was determined from this time point on for at least 7 h.

### 2.4 Resting cell bioconversions

The cells were cultivated as described above, harvested by centrifugation (10 min, 5,000 g, RT), and re-suspended to a specific cell concentration in 100 mM potassium phosphate buffer (pH 7.4) supplemented with 1 % (w/v) glucose (KPi-g buffer). The cells were transferred to baffled Erlenmeyer flasks (100 mL) or microcentrifuge tubes (2 mL) with liquid volumes of 10 or 1 mL, respectively, equilibrated at 30 °C for 10 min (flasks in a water bath at 250 rpm; microcentrifuge tubes in a ThermoMixer® C (Eppendorf, Hamburg) at 2,000 rpm), then provided with the substrate (as stated in the Table and Figure legends). Biotransformations were stopped by the addition of 0.5 mL ice-cold diethyl ether containing 0.2 mM n-decane as an internal standard to 1 mL sample. After 2 min extraction by vortexing and short centrifugation, the organic phase was dried over water-free Na<sub>2</sub>SO<sub>4</sub> before it was transferred to a GC vial for analysis. The aqueous phase was removed with a syringe from the microcentrifuge tube and stored at -20 °C for HPLC analysis.

For the conversion of 5 mM cyclohexane, 250 mL baffled Erlenmeyer flasks were used with a liquid volume of 40 mL. The caps contained two septa, a Teflon septum facing the inner side of the flask, and a silicon septum facing outwards. Pure cyclohexane (21.8 µL) was added to start the reaction. For each sampling point, 1.5 mL liquid volume was removed through the septa using a syringe. From this sample, 1 mL was extracted with diethyl ether for GC analysis as described above and 0.5 mL was used for HPLC analysis.

For details on analytical methods refer to Supplementary Information (Section 3).

### 3 Results

The construction of an efficient biocatalytic *in vivo* cascade necessitates a balanced expression of the cascade genes to avoid side product accumulation. Besides the well-characterized initiating Cyp<sup>[18, 21]</sup>, CDH and CHMO have been employed for PCL monomer synthesis from cyclohexane <sup>[16]</sup>, but nothing is known about respective reaction kinetics and possible inhibitions by pathway intermediates as they have been observed before, e.g., for Bayer-Villiger monooxygenases <sup>[22, 23]</sup>. Consequently, CDH and CHMO were characterized as the first step in this study to support the rational engineering of a productive 3-step cascade based on the optimized Cyp-containing whole-cell biocatalyst<sup>[18]</sup>.

#### 3.1 Characterization of CDH and CHMO

CDH and CHMO were cloned separately into the pSEVA244\_T vector<sup>[18]</sup> to characterize their *in vivo* activity. As CDH catalyzes an equilibrium reaction, the kinetic parameters were assayed for both reaction directions (Table 1). For the reverse reaction with cyclohexanone as substrate, CDH showed a 10 times lower  $V_{\max}$  compared to the forward reaction. On the other hand, the  $K_S$  values differed by a factor of almost 100 in favor of the reverse reaction (0.05 and 3.57 mM for cyclohexanol and cyclohexanone, respectively). Furthermore, we theoretically and experimentally assessed the cyclohexanol/cyclohexanone concentration ratio at equilibrium. Utilizing the group contribution method<sup>[24]</sup> assuming a physiological intracellular NADH to NAD concentration ratio of 10.6 under aerobic conditions<sup>[25]</sup>, this ratio was determined to be 1.9 (Supplementary Information, Section 4). It was confirmed experimentally by applying different initial alcohol and ketone concentrations giving a cyclohexanol/cyclohexanone concentration ratio of  $1.95 \pm 0.29$  after 16 h (Figure S2). This thermodynamic preference of the backward reaction, together with the low  $K_S$  value for cyclohexanone emphasizes the necessity of an efficient cyclohexanone withdrawal by the successive enzyme in the cascade, i.e., CHMO.

Substantial research has been conducted with a cyclohexanone monooxygenase originating from *Acinetobacter* sp.<sup>[26]</sup>. Generally, the substrate as well as product toxicity, are features of Baeyer-Villiger monooxygenase-catalyzed reactions <sup>[22, 23]</sup>. Substrate toxicity was generally observed at aqueous concentrations in the mM-range, which should thus be avoided during the cascade reaction. Furthermore, CHMO may be inhibited by the cascade intermediate cyclohexanol and its product  $\epsilon$ -CL. *Acidovorax* CHMO indeed was found to be highly prone to inhibition by cyclohexanol (Figure 2A). At a cyclohexanol concentration as low as 0.4 mM, the high initial CHMO activity of  $160.3 \pm 0.1 \text{ U g}_{\text{CDW}}^{-1}$  was found to be reduced to half this rate. Cyclohexanol concentrations [?] 1.7 mM completely abolished CHMO activity. However, up to an  $\epsilon$ -CL concentration of 17 mM, no product inhibition was found for CHMO (Figure 2B).

Summing up, these results emphasize that the produced cyclohexanol needs to be directly converted by CDH to avoid CHMO inhibition. High intracellular CDH and CHMO activities are important to avoid any accumulation of alcohol and ketone intermediates, as already low alcohol amounts can be expected to inherently reinforce such accumulation.

### 3.2 Assembling caprolactone-producing strains

To assess CDH and CHMO gene expression to different levels, we generated two  $\epsilon$ -CL producers based on the platform organism for Cyp gene expression developed recently [18]. First, CDH and CHMO genes were placed downstream of the Cyp genes on the same operon in *P. taiwanensis* VLB120 pSEVA\_CL\_1 (Figure 3A). Consequently, one mRNA is produced, harboring all 5 genes sequentially. To enhance CDH and CHMO levels, a second strain harboring pSEVA\_CL\_2 was created. pSEVA\_CL\_2 contains a second  $P_{trc}$  promoter upstream of the CDH and CHMO genes giving rise to increased expression rates of the respective genes.

In bioconversions applying resting *P. taiwanensis* VLB120 (pSEVA\_CL\_1),  $\epsilon$ -CL accumulated up to  $1.46 \pm 0.01$  mM within 120 min, after which the reaction was stopped (Figure 3B). Besides the desired product  $\epsilon$ -CL, also the intermediate cyclohexanol was detected to a maximal concentration of 42  $\mu$ M after 60 min. Additionally, 6HA, the hydrolysis product of  $\epsilon$ -CL (Figure 1), accumulated in the culture (especially in the second hour of bioconversion) and reached a final concentration of  $0.77 \pm 0.07$  mM after 120 min. The specific overall product formation rate considering  $\epsilon$ -CL and 6HA remained quite stable at a high level ( $37.3 \pm 1.9$  U g<sub>CDW</sub><sup>-1</sup>). The same experiment employing *P. taiwanensis* VLB120 (pSEVA\_CL\_2) (Figure 3D), resulted in  $\epsilon$ -CL accumulation to a 20 % higher concentration of  $1.80 \pm 0.01$  mM after 120 min and a higher specific product formation rate ( $43.4 \pm 1.9$  U g<sub>CDW</sub><sup>-1</sup>). In contrast to pSEVA\_CL\_1, the insertion of the second promoter completely prevented the emergence of cyclohexanol, whereas 6HA accumulated to a comparable concentration of 0.7 mM within 120 min. The activity increase observed in the first 10 min of both experiments (Figure 3BD) may be attributed to the direct addition of liquid cyclohexane into the bacterial culture resulting in high local and thus toxic/inhibitory cyclohexane concentrations, which then were attenuated upon cyclohexane redistribution among gas and liquid phase.

The direct comparison of both strains carrying either pSEVA\_CL\_1 or pSEVA\_CL\_2 via SDS-PAGE showed that Cyp levels were similar (Figure 3CE). CDH and CHMO levels were close to the detection limit in *P. taiwanensis* VLB120 (pSEVA\_CL\_1), whereas the insertion of the second promoter in the construct pSEVA\_CL\_2 significantly enhanced CDH and CHMO levels (Figure 3E). Assessing the initial specific activities of pSEVA\_CL\_1 containing enzymes for cyclohexane (37 U g<sub>CDW</sub><sup>-1</sup>), cyclohexanol (39 U g<sub>CDW</sub><sup>-1</sup>), and cyclohexanone (44 U g<sub>CDW</sub><sup>-1</sup>) conversion revealed similar values for all three reaction steps (Table 2) with the CHMO activity being slightly higher than the other two. The higher CDH and CHMO content of *P. taiwanensis* VLB120 (pSEVA\_CL\_2) directly translated into higher alcohol (76 U g<sub>CDW</sub><sup>-1</sup>) and ketone (84 U g<sub>CDW</sub><sup>-1</sup>) conversion activities, respectively (Table 2). The introduction of the second promoter doubled the CDH and CHMO activities without affecting the amount of active Cyp in the cells (Table S4). Coexpression of CDH and CHMO together with Cyp genes resulted in a 20 % growth rate reduction from  $0.37 \pm 0.01$  (pSEVA\_Cyp) to  $0.29 \pm 0.01$  h<sup>-1</sup> (pSEVA\_CL\_1), indicating a metabolic burden (Table S4). Concomitantly, the active Cyp content decreased by 30 %. Interestingly, such decreases in growth rate and active Cyp content were not observed with pSEVA\_CL\_2 (Table S4). These results indicate that higher CDH and CHMO levels are crucial to prevent the accumulation of cascade intermediates, especially of the CHMO inhibitor cyclohexanol, and thus to drive the cascade towards  $\epsilon$ -CL formation. Furthermore, the two-operon approach reduced the metabolic burden as indicated by the growth rate of the respective strain compared to the one-operon approach.

To further characterize cyclohexanol conversion efficiencies, different cyclohexanol concentrations were added to *P. taiwanensis* VLB120 cells containing pSEVA\_CL\_1 or pSEVA\_CL\_2 (Figure 3F). With pSEVA\_CL\_1, increasing cyclohexanol led to a decrease in the initial specific  $\epsilon$ -CL formation rate and the accumulation of cyclohexanone in the culture (Figure 3F). This correlated with CHMO inhibition and only 15 % of the produced cyclohexanone were converted to  $\epsilon$ -CL when 1 mM of cyclohexanol was added as substrate. For a similar cyclohexanol amount (1mM), the elevated CDH and CHMO levels in cells carrying the pSEVA.-

CL<sub>2</sub> construct resulted in a stable activity of the overall cascade, giving rise to higher cyclohexanol and, subsequently, cyclohexanone conversion with 35 % being converted to  $\epsilon$ -CL (Figure 3F). Cyclohexanone accumulation was only observed for initial cyclohexanol concentrations of [?] 0.4 mM.

In conclusion, both tested strains exhibited decent specific whole-cell activities for the entire cascade. The main difference consisted in the production of small amounts of cyclohexanol with pSEVA\_CL1. Due to CHMO inhibition and CDH kinetics, cyclohexanol was found to potentially disrupt the cascade in a self-enforcing manner. However, the high CDH and CHMO expression levels in *P. taiwanensis* VLB 120 (pSEVA\_CL2) efficiently prevented cyclohexanol accumulation. Furthermore, the two-operon approach involved a lower metabolic burden, auguring for stable biocatalytic activities.

### 3.3 Construction and characterization of a 6HA producing strain

Whereas *P. taiwanensis* VLB 120 (pSEVA\_CL2) showed promising properties regarding cascade activity and stability, the presence of host-intrinsic hydrolases still led to a product mix consisting of  $\epsilon$ -CL and 6HA (Figure 3BD). An industrial production process always relies on an efficient DSP, which in turn demands the avoidance of excessive byproduct accumulation. One possibility to prevent  $\epsilon$ -CL hydrolysis is the knockout of the respective hydrolase(s) in the host strain *P. taiwanensis* VLB120. However, its genome encodes over 100 enzymes with hydrolytic activity. Consequently, identification and inactivation of the responsible enzyme(s) would be very challenging, especially as several enzymes may be involved in this reaction, possibly even in a cooperative manner. The more promising alternative is to focus on 6HA as the only reaction product, which can also serve as a monomer to produce PCL [12]. Furthermore, 6HA is significantly less toxic to the cells as compared to  $\epsilon$ -CL (Figure 4D).

Whereas concentrations of up to 20 mM 6HA did barely affect the growth, 20 mM  $\epsilon$ -CL reduced the growth rate by ~50%. For 6HA, a half-maximal growth rate was observed at ~ 100 mM, which in turn led to complete growth inhibition in the case of  $\epsilon$ -CL.

To push the reaction towards 6HA, an additional lactonase was included in the pSEVA\_CL2 construct, originating from the cyclohexane degradation pathway of *Acidovorax* sp. CHX100 (see Supplementary Information, Section 5, for the nucleotide sequence), resulting in pSEVA\_6HA\_2 (Figure 4A). This construct indeed enabled the exclusive production of 6HA to a concentration of  $1.74 \pm 0.17$  mM after 2 h of reaction (Figure 4B). The high initial specific activity of  $52.5 \pm 5.0$  U g<sub>CDW</sub><sup>-1</sup> (in the first 5 min) dropped by 50 % within 30 min and then remained stable. Lactonase gene expression led to a detectable lactonase band and was found to enable a high  $\epsilon$ -CL hydrolysis activity of  $836.6 \pm 16.5$  U g<sub>CDW</sub><sup>-1</sup>, but did not influence Cyp, CDH, or CHMO levels and activities nor the active Cyp concentration (Figure 4C, Tables 2 and S4). The growth rate during expression ( $0.37 \pm 0.01$  h<sup>-1</sup>) also remained comparable to that of the empty vector control (Table S4). A construct pSEVA\_6HA\_1 with all genes under the control of only one promoter also was established. It again led to less favorable properties such as slower growth, (transient) cyclohexanol accumulation, and lower initial activities (Tables 2 and S4, Figure S3), confirming the superiority of the two promoter approach.

Finally, the two strains containing two-promoter constructs for the 3- or 4-step pathway were tested for the conversion of 5 mM cyclohexane on a 40 mL scale. Both strains enabled complete conversion within 3 h with the 4-step pathway being superior regarding selectivity (100 % for 6HA) than the 3-step pathway (80 % towards  $\epsilon$ -CL) (Figure 4E). The initial specific activities of *P. taiwanensis* VLB120 harboring pSEVA\_CL2 or pSEVA\_6HA\_2 were high and in the same range ( $68.4 \pm 6.5$  or  $61.5 \pm 3.2$  U g<sub>CDW</sub><sup>-1</sup>, respectively). The activities showed a decrease over time, most probably due to the decreasing substrate availability, giving overall activities of  $30.8 \pm 5.8$  and  $33.2 \pm 0.7$  U g<sub>CDW</sub><sup>-1</sup>, respectively. Consequently, complete conversion of cyclohexane to 6HA via the *in vivo* 4-step cascade was found to be feasible and efficient without serious impediments by enzyme kinetics or biocatalyst instability.

Overall, *P. taiwanensis* VLB120 (pSEVA\_6HA\_2) can be considered a highly promising production strain for the conversion of cyclohexane to the PCL monomer 6HA.

## 4 Discussion

The development of eco-efficient sustainable production processes has been one of the major objectives of biotechnology research over the last decade. Such promise is based on the inherent biodegradability, selectivity, and specificity of biocatalysts [27]. Biotechnological solutions already have replaced chemical processes for the production of biosurfactants, amino acids, and even complex heterocyclic compounds [28, 29]. The research presented in this study aimed to set a basis for the replacement of the highly polluting UCC process [13] by developing a biocatalytic synthesis route for PCL monomers.

### 4.1 Efficient design of *in vivo* cascades

We developed a production strain harboring an efficient cascade for the conversion of cyclohexane to 6HA with a decent activity in the 50-60 U g<sub>CDW</sub><sup>-1</sup> range. It has been shown that detailed analyses of enzyme kinetics and respective reaction engineering for a three-step cascade could efficiently enhance the conversion of several unsaturated cyclic alcohols to the corresponding lactones *in vitro* [1, 30]. Scherkuset *al.* analyzed the kinetic parameters of an alcohol dehydrogenase and a CHMO to produce 6HA from cyclohexanol [31]. Similarly to the CDH investigated in our study, the K<sub>M</sub> value was significantly higher for the reverse reaction, and CHMO was severely inhibited by cyclohexanol. Establishing a kinetic model enabled the setup of an efficient fed-batch process.

Whereas the balancing of enzyme ratios *in vitro* is a rather straight-forward approach [1], in case of whole-cell biocatalysis, this requires fine-tuning of expression levels which, furthermore, should not drive the demand of resources beyond cellular capacities [7]. The so-called metabolic burden arises from the change in demand for (biomass) building blocks and energy (ATP, NAD(P)H) and is system- and condition-dependent [32, 33]. In this study, we observed a gradual decrease in the growth rate with increasing operon size (Table S4). For the cascade investigated, the two-operon- compared to the one-operon approach not only enabled faster growth indicating low metabolic burden, but also led to higher CDH and CHMO expression levels and cascade activities. The relation between gene organization and gene expression is poorly understood. It has been found for *E. coli* that gene expression increases with the length of the operon resulting in more cotranscriptional translation [34]. Increased translation can result in metabolic burden and misfolded or otherwise non-functional proteins, which was found for the Cyp in our previous study [18]. Although without a terminator after the Cyp genes (Figure 3A), RNA polymerase dissociation may have been promoted by the transcription initiation machinery occupying the downstream promoter region and thereby opening up the DNA [33]. Thus, mRNAs with shorter average length can be expected for the two promoters- as compared to the one promoter constructs. Shorter mRNAs, in turn, have been found to show increased stability in *E. coli* cells [35] and to recruit fewer ribosomes [34], thus decreasing the metabolic burden. In general, the metabolic burden increases with gene and operon size and with the plasmid copy number. It is further enhanced by some antibiotics such as kanamycin and thus tends to be high for plasmid-based expression, especially when antibiotic resistance genes are used as selection markers [36]. The two operon approach may have profited from shorter but more stable mRNAs and thus reducing metabolic burden and can be considered suitable for efficient expression of the designed pathways in *P. taiwanensis* VLB120. For further optimization, metabolic modeling of cascades and combinatorial pathway engineering taking into account metabolic burden effects may become interesting, although they still suffer from incomplete knowledge [37-39].

### 4.2 Production of PCL precursors

The biocatalytic production of PCL or its precursors has been heavily investigated over the last years (Table 3). Approaches based on isolated enzymes, [15, 40-44] as well as whole cells, [16, 45-47] have successfully been established. However, most of these approaches relied on cyclohexanol as a substrate [41-47], which needs to be synthesized from cyclohexane employing an ecologically critical process [48]. Additionally, inhibition of CHMO by cyclohexanol or substrate inhibition necessitated the development of suitable reaction concepts, e.g., two-liquid phase [40] or fed-batch systems [43]. The highest productivity of 1.87 g L<sup>-1</sup> h<sup>-1</sup> was obtained with isolated enzymes by employing an appropriate feeding strategy for the complete conversion of 283 mM cyclohexanol to 6HA [43] (Table 3). The CHMO from *Acinetobacter* heterologously expressed in *E. coli* showed

the highest total turnover number (TTN) with almost 70,000 mol $\epsilon$ -CL/mol $\text{CHMO}^{-1}$  [46]. In general, whole-cell approaches show lower yields on biocatalyst, as target enzymes constitute only about 1-10% (w/w) of cells, but avoid the enormous effort to purify the enzymes.

Compared to cyclohexanol, cyclohexane is an even more challenging substrate due to its high volatility and toxicity. In comparison to solvent-sensitive *E. coli* employed to convert cyclohexanol to 6HA [47], we obtained a 10-fold higher specific whole-cell activity and a similar yield on biocatalyst (Table 3). *P. taiwanensis* VLB120 is known to tolerate low-logP solvents and can, therefore, be considered suitable for the biotransformation of the more toxic substrate cyclohexane [49, 50]. Possible prolongation of the reaction with an appropriate substrate feeding and the application of a high-cell density setup hold big potential to further improve the product titer and the volumetric productivity.

This study, for the first time, demonstrates a whole-cell approach directly converting cyclohexane to the PCL precursor 6HA. The biotransformation to  $\epsilon$ -CL presented by Karande *et al.* [16] could be optimized by enhancing the conversion, yield on biocatalyst, TTN, and specific activity (Table 3). The use of isolated enzymes to convert cyclohexane to  $\epsilon$ -CL suffered from low conversion and TTN, which can be attributed to mass transfer limitations or inherent instability of P450 monooxygenases [7, 15]. The cellular environment allows for more stable catalytic activities with superior productivities. Efficient cyclohexane mass transfer without cell toxification will constitute a major future challenge and may be solved by cyclohexane feeding potentially via the gas phase. The achieved increase in whole-cell activity and conversion is a huge step forward towards the establishment of an economically viable process [51].

### 4.3 Conclusion

In this study, we developed the strain *P. taiwanensis* VLB120 (pSEVA\_6HA\_2) that expresses 6 genes encoding 4 enzymes able to fully convert 5 mM cyclohexane to the PCL monomer 6HA. Accumulation of intermediates and byproducts was successfully prevented, and a high cascade activity was achieved. The constructed orthogonal pathway/ cascade also can serve as a template to be amended by additional enzymes to synthesize nylon monomers such as adipic acid and 6-aminohexanoic acid. This in combination with their solvent tolerance and versatility regarding reactor setups – including biofilm approaches [52] – qualify VLB120 strains harboring pSEVA\_CL\_2 or pSEVA\_6HA\_2 as promising platform organism.

### Acknowledgment

We are grateful to Andreas Schmid for helpful discussions. The authors acknowledge the use of the facilities of the Centre for Biocatalysis (MiKat) at the Helmholtz Centre for Environmental Research, which is supported by European Regional Development Funds (EFRE, Europe funds Saxony) and the Helmholtz Association. LS was funded from the ERA-IB- Project PolyBugs ID:16006 and the Sächsisches Ministerium für Wissenschaft und Kunst (SMWK) Project ID: 100318259.

### Conflict of interest

The authors declare no commercial or financial conflict of interest.

### 5 References

- [1] J. Muschiol, C. Peters, N. Oberleitner, M. D. Mihovilovic, U. T. Bornscheuer, F. Rudroff. *ChemComm* **2015** , 51 , 5798-5811.
- [2] N. Oberleitner, C. Peters, J. Muschiol, M. Kadow, S. Saß, T. Bayer, P. Schaaf, N. Iqbal, F. Rudroff, M. D. Mihovilovic. *ChemCatChem* **2013** , 5 , 3524-3528.
- [3] N. Ladkau, A. Schmid, B. Bühler. *Curr. Opin. Biotechnol.* **2014** , 30 , 178-189.
- [4] W. Szymanski, C. P. Postema, C. Tarabiono, F. Berthiol, L. Campbell-Verduyn, S. de Wildeman, J. G. de Vries, B. L. Feringa, D. B. Janssen. *Adv. Synth. Catal.* **2010** , 352 , 2111-2115.
- [5] J. H. Schrittwieser, S. Velikogne, M. I. Hall, W. Kroutil. *Chem. Rev.* **2017** , 118 , 270-348.

- [6] T. Bayer, S. Milker, T. Wiesinger, F. Rudroff, M. D. Mihovilovic. *Adv. Synth. Catal.* **2015** , 357 , 1587-1618.
- [7] M. Kadisch, C. Willrodt, M. Hillen, B. Buhler, A. Schmid. *Biotechnol. J.* **2017** , 12 , 1600170.
- [8] N. Ladkau, M. Assmann, M. Schrewe, M. K. Julsing, A. Schmid, B. Buhler. *Metab. Eng.* **2016** , 36 , 1-9.
- [9] M. Schrewe, M. K. Julsing, B. Buhler, A. Schmid. *Chem. Soc. Rev.* **2013** , 42 , 6346-6377.
- [10] M. Schrewe, M. K. Julsing, K. Lange, E. Czarnotta, A. Schmid, B. Buhler. *Biotechnol. Bioeng.* **2014** , 111 , 1820-1830.
- [11] C. K. Williams. *Chem. Soc. Rev.* **2007** , 36 , 1573-1580.
- [12] M. Labet, W. Thielemans. *Chem. Soc. Rev.* **2009** , 38 , 3484-3504.
- [13] K. Weissmermel, H.-J. Arpe, Components for Polyamides, in: Weissmermel, K., Arpe, H.-J. (Eds.), *Industrial Organic Chemistry, Fourth Edition* WILEY-VCH Verlag GmbH & Co. KGaA, Weinheim 2003, pp. 239-266.
- [14] U. Schuchardt, D. Cardoso, R. Sercheli, R. Pereira, R. S. da Cruz, M. C. Guerreiro, D. Mandelli, E. V. Spinace, E. L. Pires. *Appl. Catal., A* **2001** , 211 , 1-17.
- [15] A. Pennec, F. Hollmann, M. S. Smit, D. J. Opperman. *ChemCatChem* **2015** , 7 , 236-239.
- [16] R. Karande, D. Salamanca, A. Schmid, K. Buehler. *Biotechnol. Bioeng.* **2017** , 115 , 312-320.
- [17] J. B. van Beilen, W. A. Duetz, A. Schmid, B. Witholt. *Trends Biotechnol.* **2003** , 21 , 170-177.
- [18] L. Schafer, R. Karande, B. Buhler. *Front. Bioeng. Biotechnol.* **2020** , 8 , 140.
- [19] J. Sambrook, D. W. Russell, *Molecular cloning: a laboratory manual* , Cold Spring Harbor Laboratory, Cold Spring Harbor, NY 2001.
- [20] S. Panke, A. Meyer, C. M. Huber, B. Witholt, M. G. Wubbolts. *Appl. Environ. Microbiol.* **1999** , 65 , 2324-2332.
- [21] D. Salamanca, R. Karande, A. Schmid, D. Dobslaw. *Appl. Microbiol. Biotechnol.* **2015** , 99 , 6889-6897.
- [22] V. Alphand, G. Carrea, R. Wohlgemuth, R. Furstoss, J. M. Woodley. *Trends Biotechnol.* **2003** , 21 , 318-323.
- [23] M. A. Delgove, M. T. Elford, K. V. Bernaerts, S. M. De Wildeman. *J. Chem. Technol. Biotechnol.* **2018** , 93 , 2131-2140.
- [24] M. L. Mavrovouniotis. *Biotechnol. Bioeng.* **1990** , 36 , 1070-1082.
- [25] M. R. Leonardo, Y. Dailly, D. P. Clark. *J. Bacteriol.* **1996** , 178 , 6013-6018.
- [26] N. A. Donoghue, D. B. Norris, P. W. Trudgill. *Eur. J. Biochem.* **1976** , 63 , 175-192.
- [27] E. Ricca, B. Brucher, J. H. Schrittwieser. *Adv. Synth. Catal.* **2011** , 353 , 2239-2262.
- [28] A. Schmid, J. Dordick, B. Hauer, A. Kiener, M. Wubbolts, B. Witholt. *Nature* **2001** , 409 , 258-268.
- [29] C. Gehring, M. Wessel, S. Schaffer, O. Thum. *ChemistryOpen* **2016** , 5 , 513-516.
- [30] N. Oberleitner, C. Peters, F. Rudroff, U. T. Bornscheuer, M. D. Mihovilovic. *J. Biotechnol.* **2014** , 192 , 393-399.
- [31] C. Scherkus, S. Schmidt, U. T. Bornscheuer, H. Groger, S. Kara, A. Liese. *Biotechnol. Bioeng.* **2017** , 114 , 1215-1221.



- [32] H. Nojiri. *Curr. Opin. Biotechnol.* **2013** ,*24* , 423-430.
- [33] C. D. Smolke, J. D. Keasling. *Biotechnol. Bioeng.***2002** , *78* , 412-424.
- [34] H. N. Lim, Y. Lee, R. Hussein. *PNAS* **2011** ,*108* , 10626-10631.
- [35] L. Feng, D.-K. Niu. *Biochem. Genet.* **2007** ,*45* , 131-137.
- [36] J. Mi, A. Sydow, F. Schempp, D. Becher, H. Schewe, J. Schrader, M. Buchhaupt. *J. Biotechnol.* **2016** , *231* , 167-173.
- [37] G. Wu, Q. Yan, J. A. Jones, Y. J. Tang, S. S. Fong, M. A. Koffas. *Trends Biotechnol.* **2016** , *34* , 652-664.
- [38] M. Jeschek, D. Gerngross, S. Panke. *Curr. Opin. Biotechnol.* **2017** , *47* , 142-151.
- [39] M. Jeschek, D. Gerngross, S. Panke. *Nat. Commun.***2016** , *7* , 11163.
- [40] A. Bornadel, R. Hatti-Kaul, F. Hollmann, S. Kara. *Tetrahedron* **2016** , *72* , 7222-7228.
- [41] F. S. Aalbers, M. W. Fraaije. *Appl. Microbiol. Biotechnol.* **2017** , *101* , 7557-7565.
- [42] S. Staudt, U. T. Bornscheuer, U. Menyes, W. Hummel, H. Groger. *Enzyme Microb. Technol.* **2013** , *53* , 288-292.
- [43] C. Scherkus, S. Schmidt, U. T. Bornscheuer, H. Groger, S. Kara, A. Liese. *ChemCatChem* **2016** , *8* , 3446-3452.
- [44] S. Schmidt, C. Scherkus, J. Muschiol, U. Menyes, T. Winkler, W. Hummel, H. Groger, A. Liese, H.-G. Herz, U. T. Bornscheuer. *Angew. Chem.* **2015** , *54* , 2784-2787.
- [45] A. Kohl, V. Srinivasamurthy, D. Bottcher, J. Kabisch, U. T. Bornscheuer. *Enzyme Microb. Technol.* **2018** , *108* , 53-58.
- [46] V. S. Srinivasamurthy, D. Bottcher, J. Engel, S. Kara, U. T. Bornscheuer. *Process Biochem.* **2020** , *88* , 22-30.
- [47] V. S. Srinivasamurthy, D. Bottcher, U. T. Bornscheuer. *Z. Naturforsch. C Bio. Sci.* **2019** , *74* , 71-76.
- [48] J. Fischer, T. Lange, R. Boehling, A. Rehfinger, E. Klemm. *Chem. Eng. Sci.* **2010** , *65* , 4866-4872.
- [49] J. Volmer, A. Schmid, B. Buhler. *Biotechnol. J.***2017** , *12* , 1600558.
- [50] J.-B. Park, B. Buhler, S. Panke, B. Witholt, A. Schmid. *Biotechnol. Bioeng.* **2007** , *98* , 1219-1229.
- [51] F. Rudroff. *Curr. Opin. Chem. Biol.* **2019** ,*49* , 84-90.
- [52] A. Hoschek, I. Heuschkel, A. Schmid, B. Buhler, R. Karande, K. Buhler. *Bioresour. Technol.* **2019** , *282* , 171-178.

**Table 1:** Kinetic parameters of *P. taiwanensis* VLB120 (pSEVA244\_CDH)<sup>a</sup>.

Substrate	V <sub>max</sub> [U g <sub>CDW</sub> <sup>-1</sup> ]	K <sub>S</sub> [mM]	k <sub>cat</sub> [s <sup>-1</sup> ] <sup>b</sup>
Cyclohexanol	296.6 ± 15.7	3.57 ± 0.26	2.74 ± 0.14
Cyclohexanone	29.5 ± 1.3	0.05 ± 0.01	0.27 ± 0.01

<sup>a</sup>) Resting cell bioconversions were performed in 2 mL microcentrifuge tubes with a liquid volume of 1 mL and a biomass concentration of 0.15 g<sub>CDW</sub> L<sup>-1</sup> for 3 min.

<sup>b</sup>) Based on an estimated 5 g CDH in 100 g total dry biomass (CDW).

**Table 2.** Specific activities of *P. taiwanensis* VLB120 containing different constructs for the conversion of

the different cascade substrates/intermediates<sup>a</sup>

Desired product	Construct	Substrate	Maximal initial activity <sup>e</sup> [U g <sub>CDW</sub> <sup>-1</sup> ]
$\epsilon$ -Caprolactone	pSEVA_CL.1	Cyclohexane <sup>b</sup>	37.3 $\pm$ 0.6
		Cyclohexanol <sup>c</sup>	38.9 $\pm$ 0.5
		Cyclohexanone <sup>d</sup>	44.1 $\pm$ 1.0
	pSEVA_CL.2	Cyclohexane <sup>b</sup>	43.4 $\pm$ 1.9
		Cyclohexanol <sup>c</sup>	76.0 $\pm$ 8.3
		Cyclohexanone <sup>d</sup>	84.1 $\pm$ 2.2
6-hydroxyhexanoic acid	pSEVA_6HA.1	Cyclohexane <sup>b</sup>	38.0 $\pm$ 0.6
		Cyclohexanol <sup>c</sup>	34.4 $\pm$ 1.6
		Cyclohexanone <sup>d</sup>	46.1 $\pm$ 2.3
	pSEVA_6HA.2	$\epsilon$ -Caprolactone <sup>d</sup>	543.8 $\pm$ 21.0
		Cyclohexane <sup>b</sup>	44.8 $\pm$ 0.2
		Cyclohexanol <sup>c</sup>	82.7 $\pm$ 3.5
		Cyclohexanone <sup>d</sup>	82.9 $\pm$ 0.8
		$\epsilon$ -Caprolactone <sup>d</sup>	836.6 $\pm$ 16.5

a) Bioconversions with 0.5 g<sub>CDW</sub> L<sup>-1</sup> of cells in Erlenmeyer flasks, 10 min assay time

b) Addition of 9.2 mM cyclohexane (180  $\mu$ M in aqueous phase), activities correspond to the first 10 min in the experiments shown in Figures 3BD, 4B, S3B.

c) Maximal activity obtained by testing different cyclohexanol concentrations (see also Figure 3F)

d) Addition of 5 mM substrate

e) Average values for the sum of  $\epsilon$ -CL and 6HA formed including standard deviations of two independent biological replicates.

**Table 3:** Comparison of biocatalytic PCL precursor synthesis approaches.

Substrate	Product	Biocatalyst	Time [h]	Conversion [%]	Productivity [g L <sup>-1</sup> h <sup>-1</sup> ]	Maximal concentration [mM]	Yield [g Product g Biocatalyst <sup>-1</sup> ]	Total turnover number [mol Product mol Biocatalyst <sup>-1</sup> ]	Activity [U mg <sup>-1</sup> or [U g <sub>CDW</sub> <sup>-1</sup> ]
Cyclohexanone	$\epsilon$ -CL	E	48	58.2 (48 h)	0.19 (24 h) 0.13 (48 h)	53	12	6,000	0.05 (24h)
				42.9 (24 h)					
Cyclohexanone	$\epsilon$ -CL	E <sup>b</sup>	24	>99	0.95	200	14.9	20,000	0.09
		C	16	100 (16 h) 80 (2 h)	0.14 (16 h) 0.91 (2 h)	20	0.23	n.c. <sup>g</sup>	13.3 (2h) 2.1 (16h)
		C	20	99.6	1.1	185	0.6	69,167 <sup>e</sup> , 38,606 <sup>d</sup>	7
	6HA	E	24	94	0.27	56.4	1.29 <sup>e</sup>	690 <sup>e</sup>	0.008 <sup>e</sup>
		C	70	84	0.8	168	0.67	n.c.	3.5
	PCL	E	20	>99	1.87	283	n.c.	n.c.	n.c.

Substrate	Product	Biocatalyst	Time [h]	Conversion [%]	Productivity [g L <sup>-1</sup> h <sup>-1</sup> ]	Maximal concentration [mM]	Yield [g Product g Biocatalyst <sup>-1</sup> ]	Total turnover number [mol Product mol Biocatalyst <sup>-1</sup> ]	Activity [U mg <sup>-1</sup> or [U g DW <sup>-1</sup> ]
Cyclohexane	ε-CL	E	48	99	n.c.	n.c.	n.c.	n.c.	n.c.
		E	6	2.8	0.1	5.2	0.85 <sup>c</sup>	822 <sup>c</sup>	0.02 <sup>c</sup>
		C	5	10	0.46	20.1 <sup>f</sup>	0.43	45,585 <sup>c</sup>	12.2 (over-all) 18.0 (initial)
	6HA	C	3	100	0.24	5.5	0.68	47,900 <sup>c</sup>	33.2 (over-all) 61.5 (initial)

- a) E=isolated enzymes, C= whole cells  
b) Fusion enzyme of ADH and CHMO  
c) Calculated referring to Cyp  
d) Calculated referring to ADH  
e) Calculated referring to CHMO  
f) Total product concentration with 6HA as a side product  
g) Not calculable

## Figures

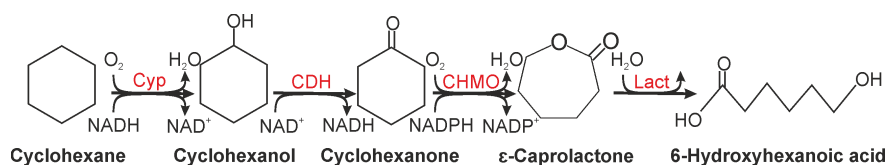


**Figure 1.** Biocatalytic cascade for the synthesis of polycaprolactone monomers. The cascade is composed of a Cytochrome P450 monooxygenase (Cyp), a cyclohexanol dehydrogenase (CDH), and a cyclohexanone monooxygenase (CHMO) for the production of ε-caprolactone (ε-CL) <sup>[16]</sup>. Optionally, a lactonase (Lact) catalyzes the ring-opening reaction to yield 6-hydroxyhexanoic acid (6HA).

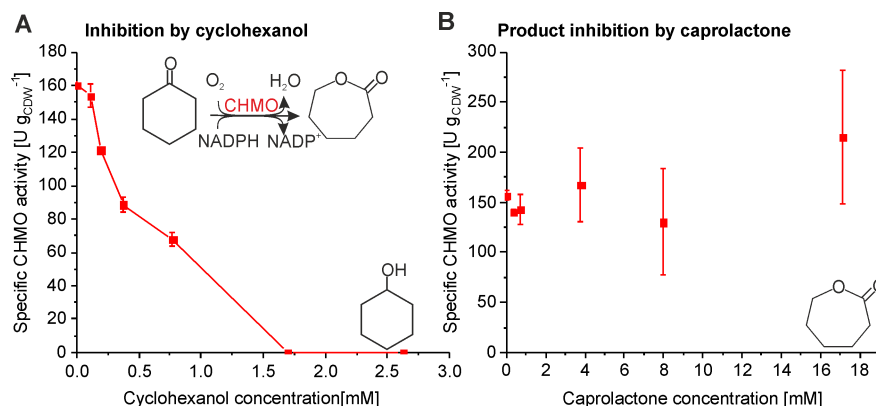


**Figure 2:** Inhibition studies with *P. taiwanensis* VLB120 (pSEVA-CHMO). The influence of cyclohexanol (A) or the product  $\epsilon$ -CL (B) on specific CHMO activity was investigated in resting cell bioconversions. Cells were cultivated in M9\* medium with 0.5 % (w/v) glucose, induced by IPTG for 6h, harvested, and resuspended in KPi-g buffer (100 mM potassium phosphate buffer supplemented with 1 % (w/v) glucose) to a biomass concentration of 0.25 g<sub>CDW</sub> L<sup>-1</sup> in 1 mL liquid volume (A) or 0.5 g<sub>CDW</sub> L<sup>-1</sup> in 10 mL liquid volume (B). Reactions were started by adding 3 mM cyclohexanone. Graphs represent average values and standard deviations of two independent biological replicates.

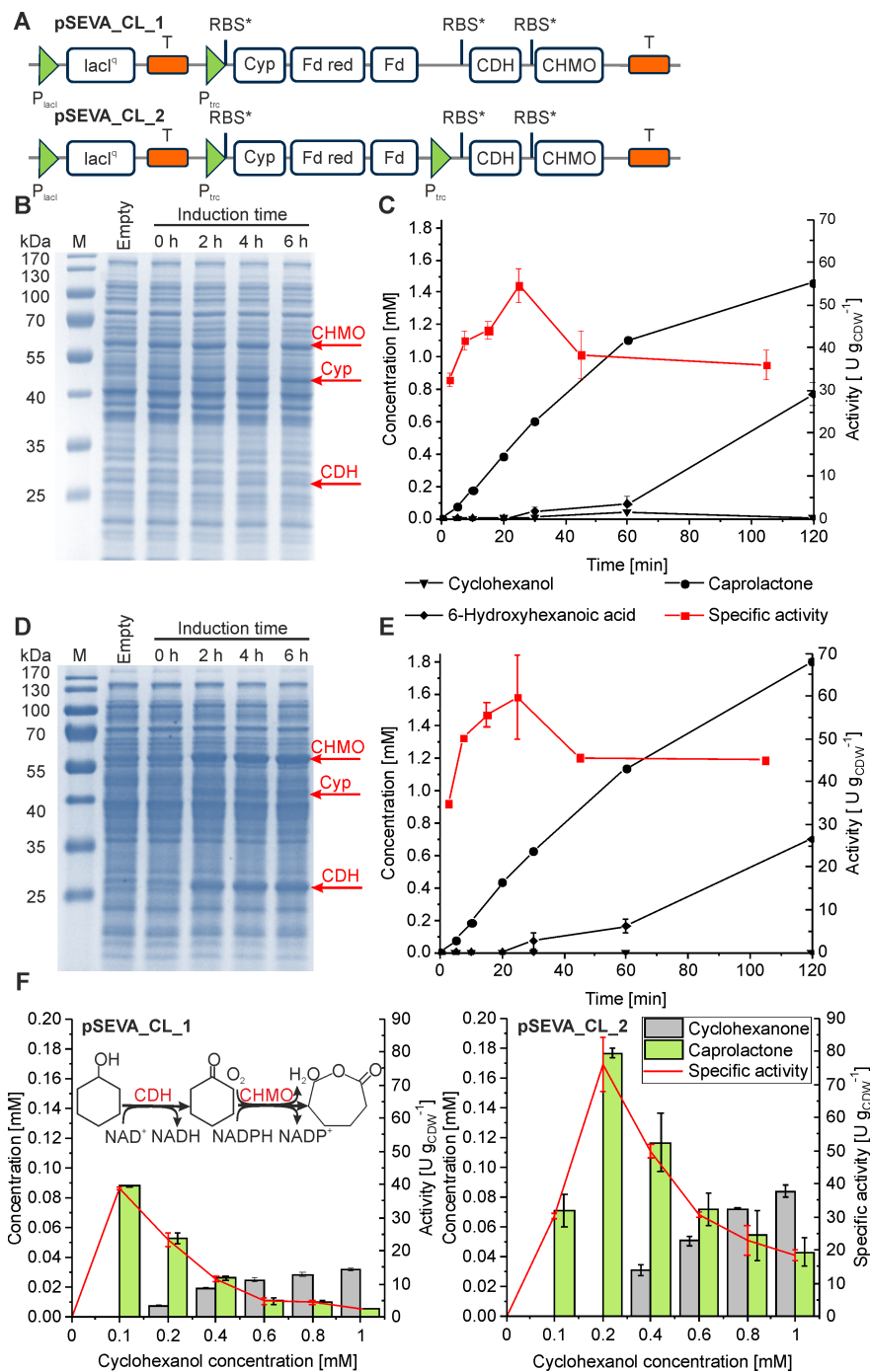


**Figure 3:** Construction and characterization of *P. taiwanensis* VLB120 pSEVA\_CL.1 (A, B, C, F) and pSEVA\_CL.2 (A, D, E, F). (A) Graphical representation of expression units in the plasmids pSEVA\_CL.1 and pSEVA\_CL.2. (B) and (D) Time courses for the production of cyclohexanol,  $\epsilon$ -CL, and 6HA and for whole-cell activities for the total product (sum of  $\epsilon$ -CL and 6HA) formation in resting cell bioconversions. Cells were cultivated as described in the legend of Figure 2 and induced for 4 h. Resting cell bioconversions were performed with a biomass concentration of  $0.5 \text{ g}_{\text{CDW}} \text{ L}^{-1}$  in 10 mL KPi-g buffer and started by adding 10  $\mu\text{L}$  of pure cyclohexane (180  $\mu\text{M}$  dissolved in the aqueous phase, 9.2 mM in total concerning the aqueous phase

volume). (C) and (E) SDS-PAGE analyses of *P. taiwanensis* VLB120 containing pSEVA.CL.1 and pSEVA.CL.2, respectively, showing bands for Cyp (47.4 kDa), CDH (26.5 kDa), and CHMO (58.8 kDa) after different times of induction and compared with cells containing an empty vector. (F) Resting cell bioconversions to study cascade inhibition by cyclohexanol. Varying cyclohexanol concentrations were applied in 1 mL KPi-g buffer with a cell concentration of  $0.25 \text{ g}_{\text{CDW}} \text{ L}^{-1}$ . The graphs depict cyclohexanone and  $\epsilon$ -CL concentrations as well as the whole-cell activity ( $\epsilon$ -CL formation) for an assay time of 10 min. Graphs represent average values and standard deviations of two independent biological replicates.

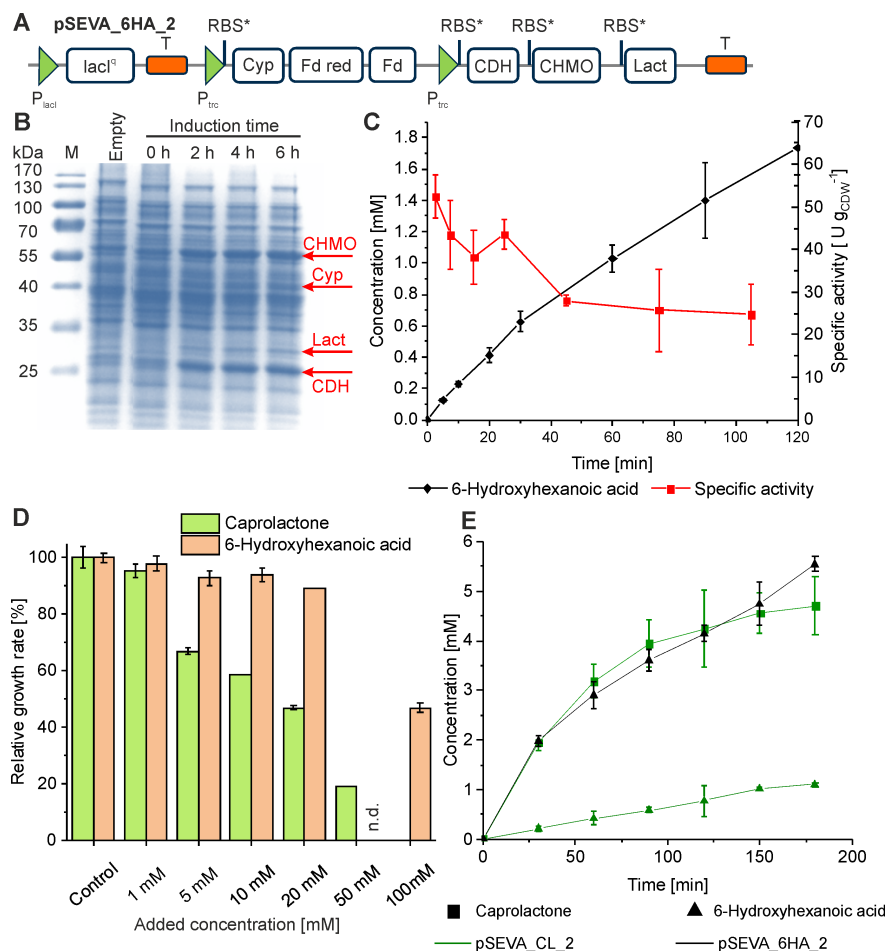


**Figure 4:** Construction and characterization of *P. taiwanensis* VLB120 (pSEVA\_6HA\_2). (A) graphical representation of expression units in the plasmid pSEVA\_6HA\_2. (B) Time courses for the 6HA concentration and the whole-cell activity for 6HA formation in resting cell bioconversions as described in the legend of Figure 3. (C) SDS-PAGE analysis showing bands for Cyp (47.4 kDa), CDH (26.5 kDa), CHMO (58.8 kDa), and Lact (32.2 kDa) after different times of induction and compared with cells containing an empty vector. (D) Relative growth rate of *P. taiwanensis* VLB120 in the presence of varying amounts of  $\epsilon$ -CL (green) or 6HA (orange) (a growth rate of  $0.47 \pm 0.01 \text{ h}^{-1}$  represents 100 %) (E) Conversion of 5 mM cyclohexane by *P. taiwanensis* VLB120 containing pSEVA.CL.2 or pSEVA.6HA.2. Resting cell bioconversions were performed in 40 mL KPi-g buffer containing  $1.05 \text{ g}_{\text{CDW}} \text{ L}^{-1}$  of cells in closed 250 mL screw-capped and baffled shake flasks. Graphs represent average values and standard deviations of two independent biological replicates.